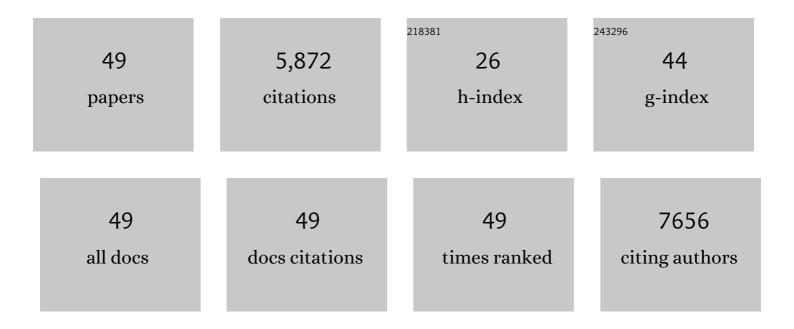
Roger P Woods

List of Publications by Year in descending order

Source: https://exaly.com/author-pdf/2241135/publications.pdf Version: 2024-02-01



#	Article	IF	CITATIONS
1	Stereotaxic white matter atlas based on diffusion tensor imaging in an ICBM template. NeuroImage, 2008, 40, 570-582.	2.1	1,528
2	Growth patterns in the developing brain detected by using continuum mechanical tensor maps. Nature, 2000, 404, 190-193.	13.7	781
3	Recovery from wernicke's aphasia: A positron emission tomographic study. Annals of Neurology, 1995, 37, 723-732.	2.8	570
4	Role of posterior parietal cortex in the recalibration of visually guided reaching. Nature, 1996, 383, 618-621.	13.7	390
5	Extending the Human Connectome Project across ages: Imaging protocols for the Lifespan Development and Aging projects. NeuroImage, 2018, 183, 972-984.	2.1	290
6	Structural Plasticity of the Hippocampus and Amygdala Induced by Electroconvulsive Therapy in Major Depression. Biological Psychiatry, 2016, 79, 282-292.	0.7	241
7	Within-arm somatotopy in human motor areas determined by positron emission tomography imaging of cerebral blood flow. Experimental Brain Research, 1993, 95, 172-6.	0.7	197
8	The Lifespan Human Connectome Project in Aging: An overview. NeuroImage, 2019, 185, 335-348.	2.1	186
9	Motion detection and correction in functional MR imaging. Human Brain Mapping, 1995, 3, 224-235.	1.9	176
10	Creation and use of a Talairach-compatible atlas for accurate, automated, nonlinear intersubject registration, and analysis of functional imaging data. Human Brain Mapping, 1999, 8, 73-79.	1.9	147
11	Widespread Cortical Thinning Is a Robust Anatomical Marker for Attention-Deficit/Hyperactivity Disorder. Journal of the American Academy of Child and Adolescent Psychiatry, 2009, 48, 1014-1022.	0.3	130
12	Normal variants of Microcephalin and ASPM do not account for brain size variability. Human Molecular Genetics, 2006, 15, 2025-2029.	1.4	115
13	Neurochemical correlates of rapid treatment response to electroconvulsive therapy in patients with major depression. Journal of Psychiatry and Neuroscience, 2017, 42, 6-16.	1.4	108
14	Principal Component Analysis and the Scaled Subprofile Model Compared to Intersubject Averaging and Statistical Parametric Mapping: I. "Functional Connectivity―of the Human Motor System Studied with [150]Water PET. Journal of Cerebral Blood Flow and Metabolism, 1995, 15, 738-753.	2.4	102
15	Characterizing volume and surface deformations in an atlas framework: theory, applications, and implementation. NeuroImage, 2003, 18, 769-788.	2.1	96
16	Effect of Electroconvulsive Therapy on Striatal Morphometry in Major Depressive Disorder. Neuropsychopharmacology, 2016, 41, 2481-2491.	2.8	74
17	Improved Detection of Focal Cerebral Blood Flow Changes Using Three-Dimensional Positron Emission Tomography. Journal of Cerebral Blood Flow and Metabolism, 1993, 13, 630-638.	2.4	59
18	Genetic variation and gene expression across multiple tissues and developmental stages in a nonhuman primate. Nature Genetics, 2017, 49, 1714-1721.	9.4	57

Roger P Woods

#	Article	IF	CITATIONS
19	Alcohol exposure in utero is associated with decreased gray matter volume in neonates. Metabolic Brain Disease, 2016, 31, 81-91.	1.4	53
20	Modulation of Intrinsic Brain Activity by Electroconvulsive Therapy in Major Depression. Biological Psychiatry: Cognitive Neuroscience and Neuroimaging, 2016, 1, 77-86.	1.1	50
21	A study of the effects of prenatal alcohol exposure on white matter microstructural integrity at birth. Acta Neuropsychiatrica, 2015, 27, 197-205.	1.0	49
22	Modulation of amygdala reactivity following rapidly acting interventions for major depression. Human Brain Mapping, 2020, 41, 1699-1710.	1.9	46
23	Mechanisms of Antidepressant Response to Electroconvulsive Therapy Studied With Perfusion Magnetic Resonance Imaging. Biological Psychiatry, 2019, 85, 466-476.	0.7	43
24	Multitracer: a Java-based tool for anatomic delineation of grayscale volumetric images. NeuroImage, 2003, 19, 1829-1834.	2.1	40
25	Desynchronization and Plasticity of Striato-frontal Connectivity in Major Depressive Disorder. Cerebral Cortex, 2016, 26, 4337-4346.	1.6	37
26	Hippocampal dysfunction during declarative memory encoding in schizophrenia and effects of genetic liability. Schizophrenia Research, 2015, 161, 357-366.	1.1	31
27	Interhemispheric Functional Brain Connectivity in Neonates with Prenatal Alcohol Exposure: Preliminary Findings. Alcoholism: Clinical and Experimental Research, 2016, 40, 113-121.	1.4	27
28	Hippocampal subregions and networks linked with antidepressant response to electroconvulsive therapy. Molecular Psychiatry, 2021, 26, 4288-4299.	4.1	25
29	Anatomy of nerve fiber bundles at micrometer-resolution in the vervet monkey visual system. ELife, 2020, 9, .	2.8	23
30	Inter and intra-hemispheric structural imaging markers predict depression relapse after electroconvulsive therapy: a multisite study. Translational Psychiatry, 2017, 7, 1270.	2.4	21
31	Modulation of the functional connectome in major depressive disorder by ketamine therapy. Psychological Medicine, 2022, 52, 2596-2605.	2.7	20
32	Metric-induced optimal embedding for intrinsic 3D shape analysis. , 2010, , .		18
33	Epigenetic clock and methylation studies in vervet monkeys. GeroScience, 2022, 44, 699-717.	2.1	18
34	Variations in Hippocampal White Matter Diffusivity Differentiate Response to Electroconvulsive Therapy in Major Depression. Biological Psychiatry: Cognitive Neuroscience and Neuroimaging, 2019, 4, 300-309.	1.1	17
35	Depressive Symptom Dimensions in Treatment-Resistant Major Depression and Their Modulation With Electroconvulsive Therapy. Journal of ECT, 2020, 36, 123-129.	0.3	12
36	Central white matter integrity alterations in 2-3-year-old children following prenatal alcohol exposure. Drug and Alcohol Dependence, 2021, 225, 108826.	1.6	12

ROGER P WOODS

#	Article	IF	CITATIONS
37	Prenatal depression exposure alters white matter integrity and neurodevelopment in early childhood. Brain Imaging and Behavior, 2022, 16, 1324-1336.	1.1	11
38	Modulation of brain networks during MR-compatible transcranial direct current stimulation. NeuroImage, 2022, 250, 118874.	2.1	11
39	Random forest classification of depression status based on subcortical brain morphometry following electroconvulsive therapy. , 2015, 2015, 92-96.		10
40	Ketamine's modulation of cerebro-cerebellar circuitry during response inhibition in major depression. NeuroImage: Clinical, 2021, 32, 102792.	1.4	10
41	Structural and functional brain network alterations in prenatal alcohol exposed neonates. Brain Imaging and Behavior, 2021, 15, 689-699.	1.1	9
42	Accounting for symptom heterogeneity can improve neuroimaging models of antidepressant response after electroconvulsive therapy. Human Brain Mapping, 2021, 42, 5322-5333.	1.9	9
43	Creation and use of a Talairach-compatible atlas for accurate, automated, nonlinear intersubject registration, and analysis of functional imaging data. , 1999, 8, 73.		6
44	Data-driven cluster selection for subcortical shape and cortical thickness predicts recovery from depressive symptoms. , 2017, 2017, 502-506.		5
45	A novel technique for accurate electrode placement over cortical targets for transcranial electrical stimulation (tES) clinical trials. Journal of Neural Engineering, 2021, 18, .	1.8	5
46	The impact of prenatal alcohol exposure on gray matter volume and cortical surface area of 2 to 3â€yearâ€old children in a South African birth cohort. Alcoholism: Clinical and Experimental Research, 2022, 46, 1233-1247.	1.4	3
47	Multimodal Data Registration for Brain Structural Association Networks. Lecture Notes in Computer Science, 2019, 11765, 373-381.	1.0	2
48	Anterior default mode network and posterior insular connectivity is predictive of depressive symptom reduction following serial ketamine infusion. Psychological Medicine, 2022, , 1-11.	2.7	2
49	Brain Network Connectivity from Matching Cortical Feature Densities. , 2020, 2020, 995-998.		Ο